Proc. NIPR Symp. Antarct. Geosci., **9**, 91–108, 1996

PRELIMINARY REPORT OF GEOPHYSICAL AND GEOLOGICAL SURVEYS OF THE WEST WILKES LAND MARGIN

Takemi ISHIHARA[1]*, Manabu TANAHASHI[2†], Mikio SATO[2] and Yoshihisa OKUDA[2]

[1]*Technology Research Center, Japan National Oil Corporation, 2–2, Uchisaiwai-cho 2-chome, Chiyoda-ku, Tokyo 100*
[2]*Geological Survey of Japan, 1–3, Higashi 1-chome, Tsukuba 305*

Abstract: Geophysical and geological surveys of the western part of the Wilkes Land margin were conducted in the 1994–95 austral summer season. The survey area covers the continental slope and rise as well as Bruce Rise in the western end of the margin.

Sediments above the basement in the survey area are divided into six sequences. The continent-ocean boundary (COB) occurs at about 64°S, and total thickness of sediments exceeds 5 s in two-way time around the COB in the eastern part of the survey area. Bottom simulating reflectors are frequently observed in the continental slope area.

A conspicuous unconformity is observed in Bruce Rise. The basement almost crops out near the northern and eastern ends of the rise, and the sequences below the unconformity dip west to southwest.

key words: Wilkes Land margin, marine geophysical and geological surveys, sedimentary sequence, bottom simulating reflector

1. Introduction

The Technology Research Center, Japan National Oil Corporation has been conducting marine geophysical and geological surveys of the Antarctic continental margins every year since 1980. Some of the results of previous survey cruises have been already published (KIMURA, 1982; OKUDA *et al.*, 1983; SATO *et al.*, 1984; TSUMURAYA *et al.*, 1985; MIZUKOSHI *et al.*, 1986; SAKI *et al.*, 1987; YAMAGUCHI *et al.*, 1988; SHIMIZU *et al.*, 1989).

According to identification of magnetic anomalies south of Australia and the Wilkes Land margin of Antarctica, oceanic spreading between Australia and Antarctica began at about 95 Ma, continued by a very slow rate of 4.5 mm/yr, then the spreading rate increased to 23 mm/yr at about 45 Ma (CANDE and MUTTER, 1982; VEEVERS, 1987). There is a topographic high, Bruce Rise, at longitude about 100°E in the western end of the Wilkes Land margin, with a top shallower than 1500 m and a diameter of approximately 100 km (Fig. 1).

*Present address: Geological Survey of Japan, 1–3, Higashi 1-chome, Tsukuba 305.
†Present address: Technology Research Center, Japan National Oil Corporation, 2–2, Uchisaiwai-cho 2-chome, Chiyoda-ku, Tokyo 100.

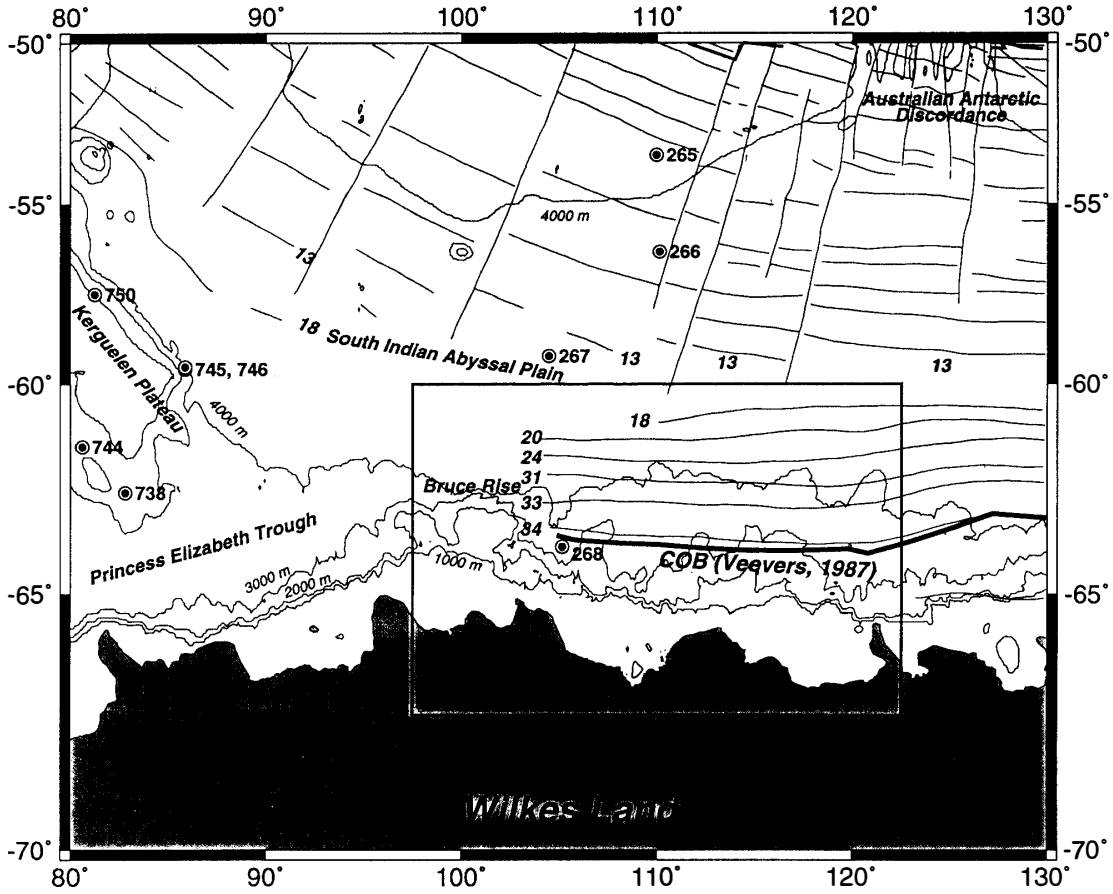

Fig. 1. Tectonic setting of the TH-94 survey area. The box shows the JNOC TH-94 survey area. Thin lines show the fracture zones and magnetic lineation pattern. These lines are drawn using data files in the NOAA National Geophysical Data Center (NGDC) Global Relief CD-ROM. Bathymetry is based on the NOAA/NGDC ETOPO5 data base. The thick line connects COB (Continent-Ocean Boundary) points given by VEEVERS (1987). Double circles with numbers show the locations of drill sites of the Deep Sea Drilling Project (DSDP) and the Ocean Drilling Program (ODP). Many figures including this one were drawn with the Generic Mapping Tools (GMT) by WESSEL and SMITH (1991).

Very limited geophysical and geological data have been obtained from the western part of the Wilkes Land margin. The TH-83 cruise was the only one during which a multichannel seismic survey was conducted (TSUMURAYA *et al.*, 1985). This paper reports the preliminary results of the TH-94 cruise.

2. Outline of Survey

Marine geophysical and geological surveys were carried out in the western part of the Wilkes Land margin by R/V HAKUREI-MARU from 21 to 31 December 1994 and from 18 January to 8 February 1995. Data acquired during this cruise are summarized in Table 1.

13293 km of gravity and magnetic data were obtained, and 2377 km of seismic reflection data were recorded with four 210 in^3 GI-guns and a 1200 m, 48 channel

Table 1. Summary of the TH-94 cruise.

Survey period	33	days
Seismic reflection survey	4244	km
Multichannel	2377	km
Single channel	1867	km
Seismic refraction survey	6	sites
Magnetic and gravity survey	13293	km
Heat flow measurement	8	sites
Gravity coring	9	sites
Dredging	4	sites

Table 2. Summary of survey instruments and specification.

Survey	Instrument and specification
Multichannel seismic reflection	Source: 4 SSI GI-guns (105 cu.in. generator+105 cu.in. injector) Receiver: 1200 m AMG 37–43 streamer cable (48 channels, 25 m interval) Recorder: TI DFS-V Record length: 6 s Sampling rate: 4 ms Shot interval: 50 m CDP coverage: 1200 %
Single channel seismic reflection	Source: SSI GI-gun Receiver: 50 Geospace MP-18-200 hydrophones Recorder: LSR-1807M
Seismic refraction	Source: 4 SSI GI-guns Receiver: DTC-6030 Ocean bottom seismometer
Gravity	Lacoste & Romberg SL-2 gravimeter
Magnetics	Geometrics G-811G proton gradiometer or Geometrics G-866 proton magnetometer
Bottom sampling	Gravity corer and dredger
Heat flow	Nichiyu Giken GS-type Thermal conductivity: Kyoto Denshi QTM-D3 type

streamer cable. Seismic refraction surveys were carried out at six sites along the seismic reflection lines. A 3.5 kHz subbottom profiler and a 12 kHz precision depth recorder were operated throughout the survey period. Sea bottom samplings were carried out at 13 sites including simultaneous terrestrial heat flow measurements at eight sites.

The survey instruments and methods are summarized in Table 2.

3. Sea Bottom Samplings and Terrestrial Heat Flow Measurements

3.1. Sea bottom samplings

Unconsolidated sediments were obtained by a gravity corer at nine sites (Fig. 2).

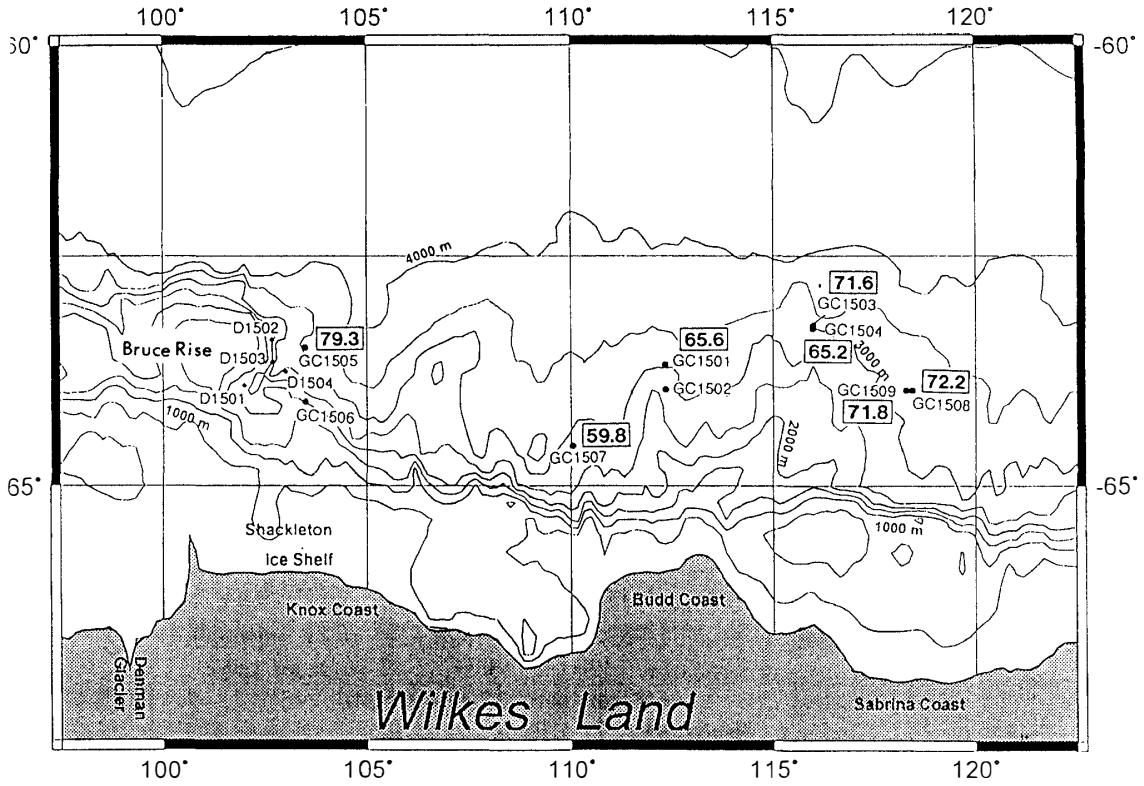

Fig. 2. Locations of sea bottom samplings. GC: gravity core; D: dredge. Numbers in boxes represent terrestrial heat flow values.

A dredger was used to collect rocks at four sites. The results of bottom samplings are summarized in Table 3. A micropaleontological study of the obtained samples was carried out. Unconsolidated sediments obtained by the dredger do not have enough fossils for the micropaleontological study.

3.1.1. Foraminiferal fossils

Planktonic foraminiferal assemblages of all the gravity cores are monospecific of *Neogloboquadrina pachyderma*, which ranges in age from Pliocene to Holocene. Lower parts of cores GC1502 and GC1504 also contain warm-water foraminifera, *Globorotaria scitula.*

Four benthonic foraminiferal assemblages are recognized in the gravity cores:
Nuttalides umbonifer - *Epistominella exigua*,
Epistominella exigua - *Pullenia* spp.,
Epistominella exigua - *Cassidulina carinata*,
and *Martinottiella antarctica* - *Cyclammina* spp.

3.1.2. Diatom fossils

Gravity cores GC1505 and GC1509 contain abundant diatom fossils in their whole cores. Diatom fossils are generally abundant in the upper part of the remaining seven cores, while they are rather rare in the lower part.

Diatom fossils can be divided into four zones of assemblages based on the diatomaceous zonation of AKIBA (1982), *i.e., Nitzschia kerguelensis* Zone (0–0.2 Ma),

Table 3. Summary of bottom samplings and heat flow measurements.

Site	Lat.(S)	Long.(E)	Depth(m)	Recovery	Description	T.C.	H.F.
GC1501	63°43′13″	112°20′06″	3060	5.40	Silic. silt	0.844	65.6
GC1502	63°59′23″	112°20′24″	2656	5.42	Silic. silt, silic. sand-silt, silty clay		
GC1503	63°17′30″	115°59′42″	3368	5.24	Silic. silt	0.858	71.6
GC1504	63°19′43″	116°00′06″	3310	5.23	Silic. sand-silt, silty clay, silty sand	0.873	65.2
GC1505	63°32′19″	103°30′24″	3607	3.71	Silic. silt, silty clay, silty sand, fine to coarse sand	0.778	79.3
GC1506	64°08′13″	103°30′00″	2048	1.14	Silic. silt, silty clay, silt		
D1501	63°56′45″	102°00′18″	2667		Sand-silt		
	63°57′00″	102°00′06″	2599				
D1502	63°27′10″	102°41′36″	2446		Semi-consilidated siltstones,		
	63°26′49″	102°41′00″	2495		granites, schists quartzose sandstone		
D1503	63°41′46″	102°43′24″	2744		Semi-consolidated siltstones,		
	63°41′28″	102°41′42″	2834		granites, schists		
D1504	63°47′28″	103°00′30″	2896		Semi-consolidated mudstones,		
	63°48′06″	103°02′36″	2668		granites, schists, quartzose sandstones		
GC1507	64°35′01″	110°02′18″	2604	4.53	Silty clay	0.865	59.8
GC1508	63°59′56″	118°26′18″	3232	5.32	Silic. clay, diatom ooze	0.819	72.2
GC1509	63°59′53″	118°17′12″	3198	5.39	Silic. clay	0.821	71.8

Recovery: Recovery length (m), T.C.: Thermal conductivity (10^{-3} cal/cm s °C), H. F.: Heat flow (mW/m^2).

Hemidiscus karstenii Zone (0.2–0.35 Ma), *Rouxia isopolica* Zone (0.35–0.62 Ma) and *Actincyclus ingens* Zone (0.62–1.67 Ma). The assemblages of diatom fossils corresponding to all of the four zones are included in gravity cores GC1501, GC1502, GC1504 and GC1508, while cores GC1505 and GC1509 contain only the upper three and two zones, respectively. The remaining three cores also comprise assemblages from the *Nitschia kerguelensis* Zone to the *Actincyclus ingens* Zone, though division into the upper three zones is difficult for core GC1503, and the *Hemidiscus karstenii* Zone (or the *Rouxia isopolica* Zone) is missing from core GC1507 (or GC1506).

3.1.3. Radiolarian fossils

Radiolarian assemblages in gravity cores GC1505, GC1506, GC1508 and GC1509 are correlated to the *Antarctica denticulata* Zone, which suggests that these cores range in age from the latest Late Pleistocene to the Recent, while those in the remaining five cores are correlated to the *Stylatractus universus* Zone and the *A. denticulata* Zone, which suggests that these cores range from the Late Pleistocene to the Recent.

3.2. Terrestrial heat flow measurements

Terrestrial heat flow data were obtained from the product of the geothermal gradient and the thermal conductivity of the sediments at seven sampling sites by the

gravity corer. The geothermal gradient was measured during the sampling operation by six sensors installed at 80 cm intervals on the corer, while the thermal conductivity of the collected samples was measured after the sampling operation.

Heat flow values of 60 to 80 mW/m^2 were obtained (Fig. 2). They are approximately equal to the world average value.

4. Gravity and Magnetic Surveys

Absolute gravity values were calculated by adjusting to IGSN71 at the port of Fremantle before the cruise and at the port of Sydney after the cruise. Free-air gravity anomalies are generally negative in the continental slope and rise areas (Fig. 3). Two topographic highs extending in a NNE direction from the Budd Coast and the Knox Coast, respectively, are associated with positive anomalies, which are probably due to the gravity effect of the thick sediments brought by glaciers. Positive anomalies corresponding to basement highs are observed in the northern and eastern parts of Bruce Rise. A gravity anomaly map derived from satellite altimetry data (SANDWELL and SMITH, 1992) also shows these features as well as conspicuous positive anomalies along the continental shelf edge.

Magnetic anomaly values were obtained by subtracting the IGRF90 reference field from the measured total magnetic field. No correction was made for diurnal variation or magnetic storms. Magnetic anomaly data collected by this cruise as well as old available data in this area are shown in Fig. 4. Tentative identification of the magnetic anomalies based on VEEVERS (1987), shows that the continent-ocean

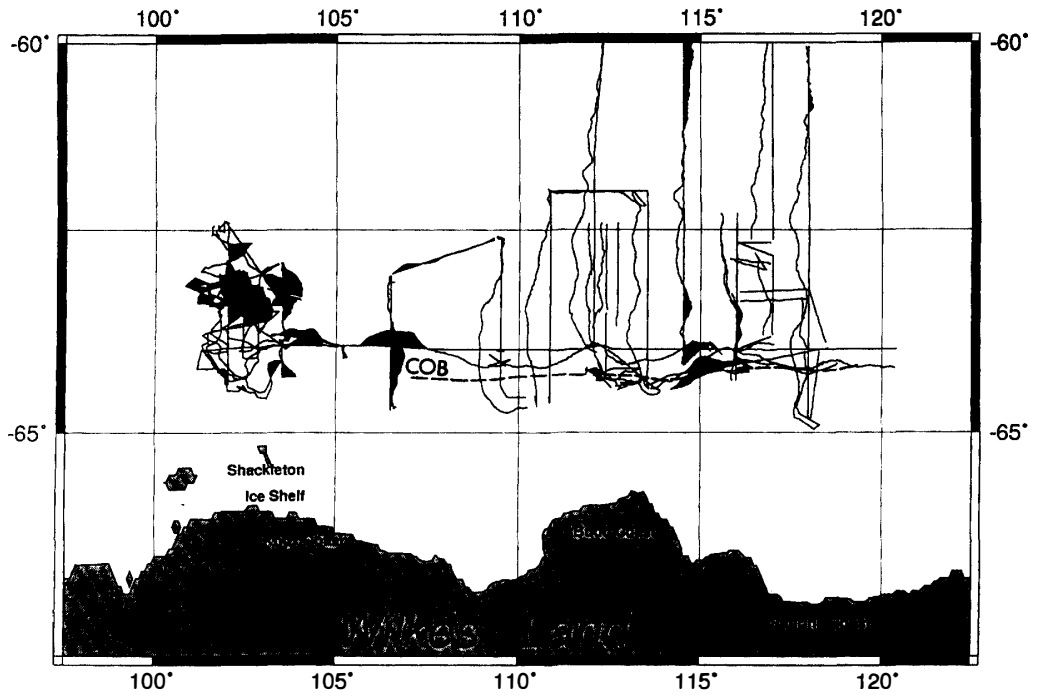

Fig. 3. Free-air gravity anomaly profiles along the ship's track. The dashed line shows the COB.

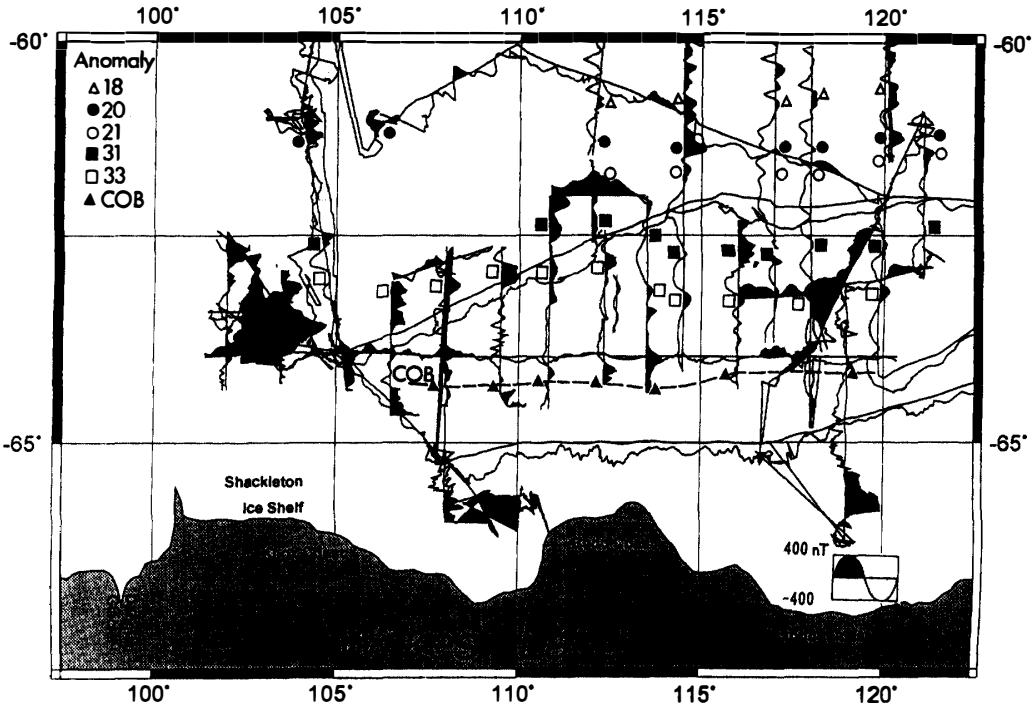

Fig. 4. Magnetic anomaly profiles along the ship's track. Data from TH-83 and ELTANIN *cruises and DSDP leg 28 are also included. Also shown are the identified sea floor spreading anomalies and the COB anomaly, based upon* VEEVERS *(1987).*

boundary (COB) lies along or slightly south of 64°S.

5. Seismic Survey

5.1. Seismic refraction survey

A seismic refraction survey was carried out using ocean bottom seismometers (OBS) deployed at six sites along seismic reflection survey lines as shown in Fig. 5. Three-component seismometer and hydrophone data were recorded. The hydrophone record section for OBS 2 along line 6SMG is shown in Fig. 6 as an example. Sufficient data for conventional refraction analysis were obtained at four sites including two data sets along different lines at site OBS5. Velocity structures derived from the analysis are illustrated in Fig. 7.

5.2. Seismic reflection survey

Seismic reflection data were collected along 13 lines including five partitioned lines along 64°S (Fig. 5). They were processed according to a conventional seismic data processing flow.

5.2.1. Mid-eastern part of the survey area

Seven seismic sequences A, B, C, D, E, F and G (acoustic basement) can be traced from top downward throughout the survey area except Bruce Rise (Table 4). In the eastern part of the Wilkes Land margin, HAMPTON *et al.* (1987) and EITTREIM and SMITH (1987) identified seismic sequences A2, A1, B2, B1, C and D. They probably correspond to our sequences A, B, C, D+E, F and G, respectively.

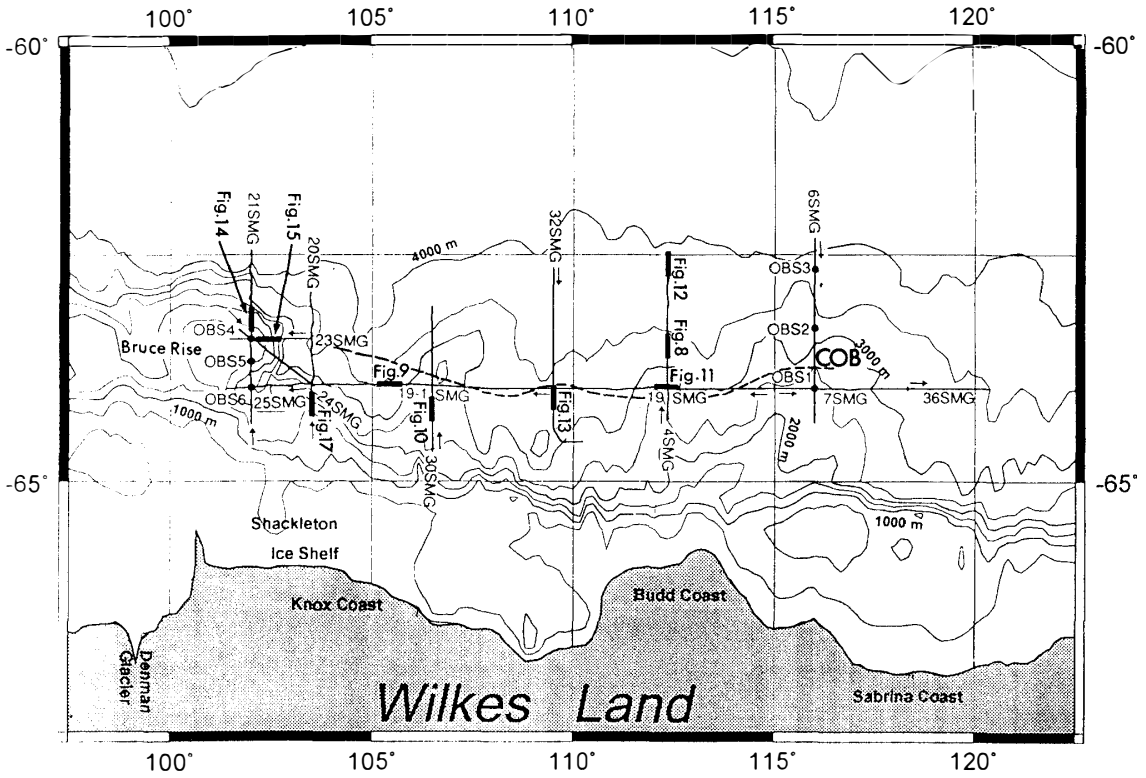

Fig. 5. Lines of the multichannel seismic reflection survey and sites of the OBS seismic refraction survey. 'Fig. 8' to 'Fig. 17' indicate parts of lines, where seismic profiles are illustrated as figures. Also shown are the COB inferred from seismic reflection characters of the basement G.

Table 4. Sequences, their maximum thicknesses and geologic time in the Wilkes Land margin.

Bruce Rise	Mid-eastern part		East Wilkes Land	Geologic time
A (0.8)	A (1.9)		A2	Quaternary-Miocene
B (0.3)	B (1.7)		A1	Oligocene-Paleocene
	C (0.8)		B2	Late Cretaceous
D (0.4)	D (0.7)		B1	
E (1.7)	E (1.0)			
F (1.3)	F (>1.7)	G (seaward of COB)	C	Early Cretaceous
G	G (landward of COB)		D	Early Cretaceous and/or older

Numbers in parentheses are maximum thicknesses in s of two-way travel time.
Sequences in east Wilkes Land are according to HAMPTON *et al.* (1987) and EITTREIM and SMITH (1987).

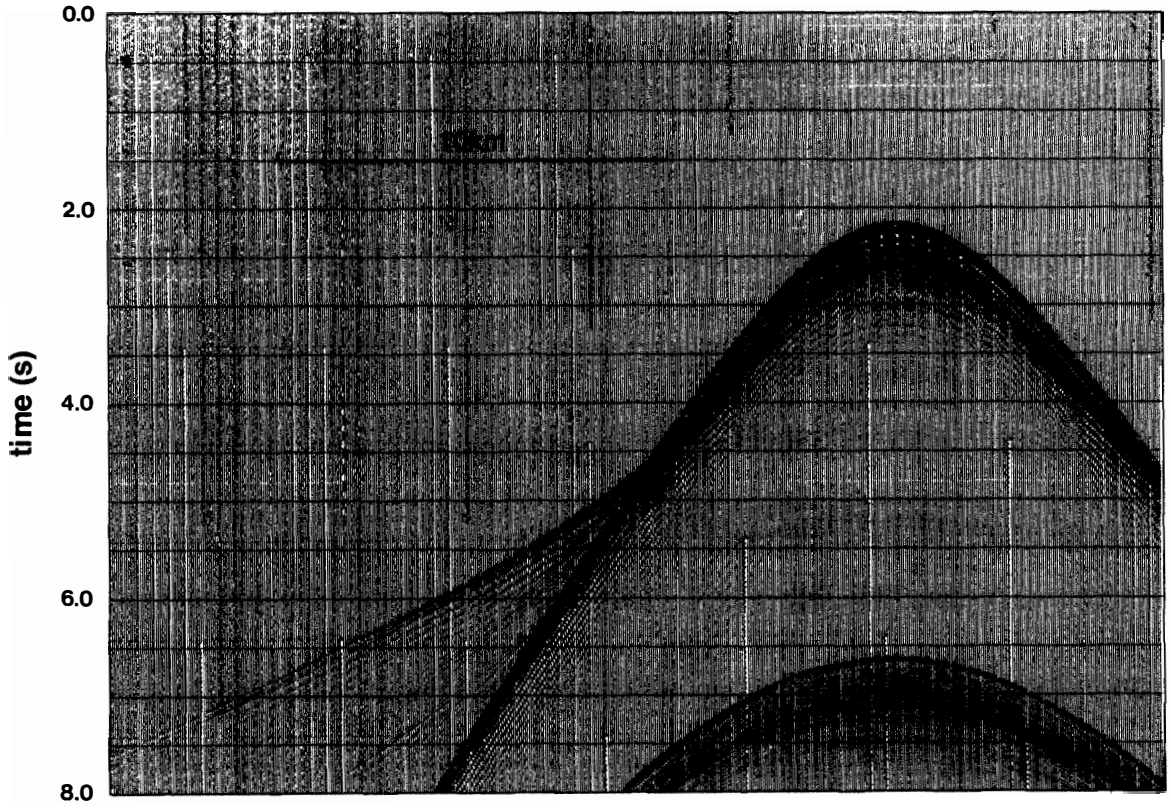

Fig. 6. Hydrophone record section for OBS2 along line 6SMG.

Seismic reflection patterns of the seven sequences are summarized as follows.

The upper part of sequence A is characterized by high amplitude reflectors with good continuity. Many interesting features are observed in places of this part: wavy reflectors (Fig. 8), erosion by submarine canyons (Figs. 9 and 10), sedimentation by turbidity current (Fig. 10), etc. The lower part of the sequence is generally characterized by lower amplitude reflectors with poor continuity. Slumping is also observed as fault planes cutting sequence A (or A and B, Fig. 11) .

Sequence B is generally characterized by clear reflectors with good continuity, and the amplitude of reflectors becomes higher with better continuity northward (*e.g.*, Figs. 8, 12 and 13).

Sequence C is characterized by very high amplitude reflectors with good continuity in the eastern part of the survey area (*e.g.*, Figs. 8, 11 and 12). The amplitude of reflectors becomes lower in the western part of the survey area (*e.g.*, Figs. 9 and 17).

Sequences D and E generally have reflectors with fairly good continuity (*e.g.*, Figs. 8, 9, 10 and 11).

Sequence F generally has no clear reflectors, which reminds us of terrigenous sedimentary rocks (*e.g.*, Figs. 8, 9, 11 and 13).

Sequence G is the acoustic basement. The sequence is characterized by strong fragmentary reflectors with hyperbolic diffractions and with large undulation in the central and northern parts of the survey area. This is probably due to volcanic

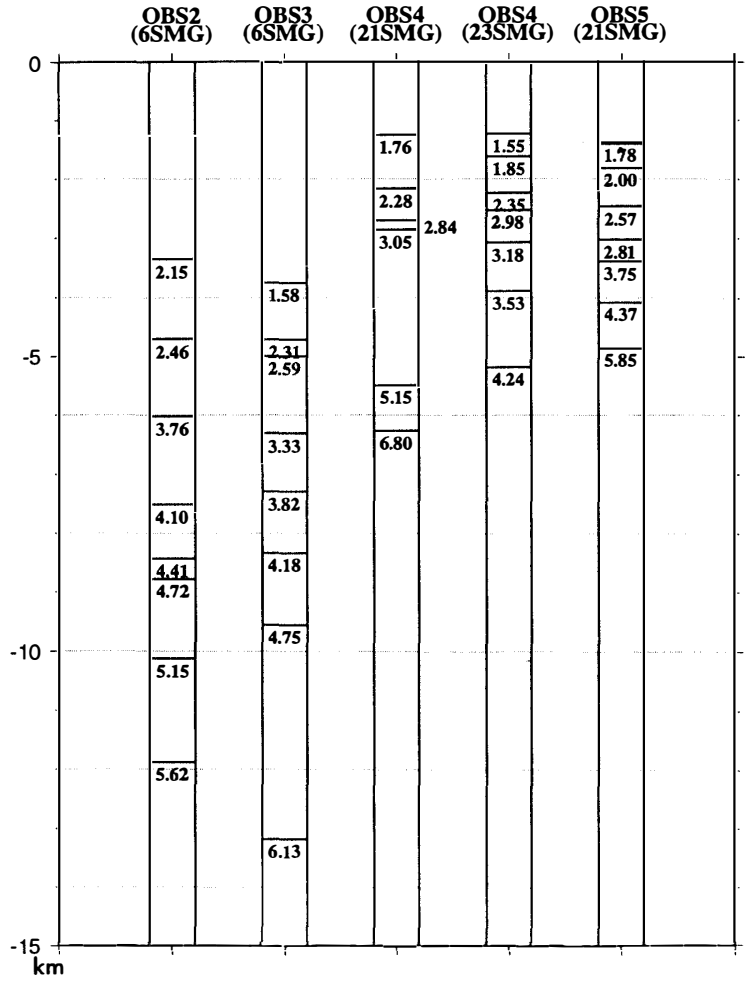

Fig. 7. Velocity-depth solutions from OBS seismic refraction survey (unit: km/s for velocity and km for depth).

materials in the oceanic crust. The basement becomes shallower northward and lacks the above sequences F, E, D and C in the northern ends of the N-S lines (Fig. 12). In the southern end of the survey area, the basement has rather low-amplitude reflectors with poor continuity (*e.g.*, Fig. 13). This probably consists of old sedimentary or metamorphic continental rocks, and the COB is considered to lie between these two different types of basement (*e.g.*, on the left side of Fig. 13). The COB line inferred from the boundary of the two types of basement lies seaward of that based on the magnetic anomaly identification (Figs. 4 and 5).

5.2.2. Bruce Rise

Sequences C and D are almost missing in Bruce Rise. Other sequences can be traced from the mid-eastern part of the survey area (Table 4). The lower sequences E, F and G dip west to southwest, and are folded and cut by faults in its northern and eastern parts (Figs. 14 and 15). These sequences are unconformably overlain by younger sequences A and B with a thickness 1 s or less in two-way travel time. The basement G almost crops out near the northern and eastern ends of the rise.

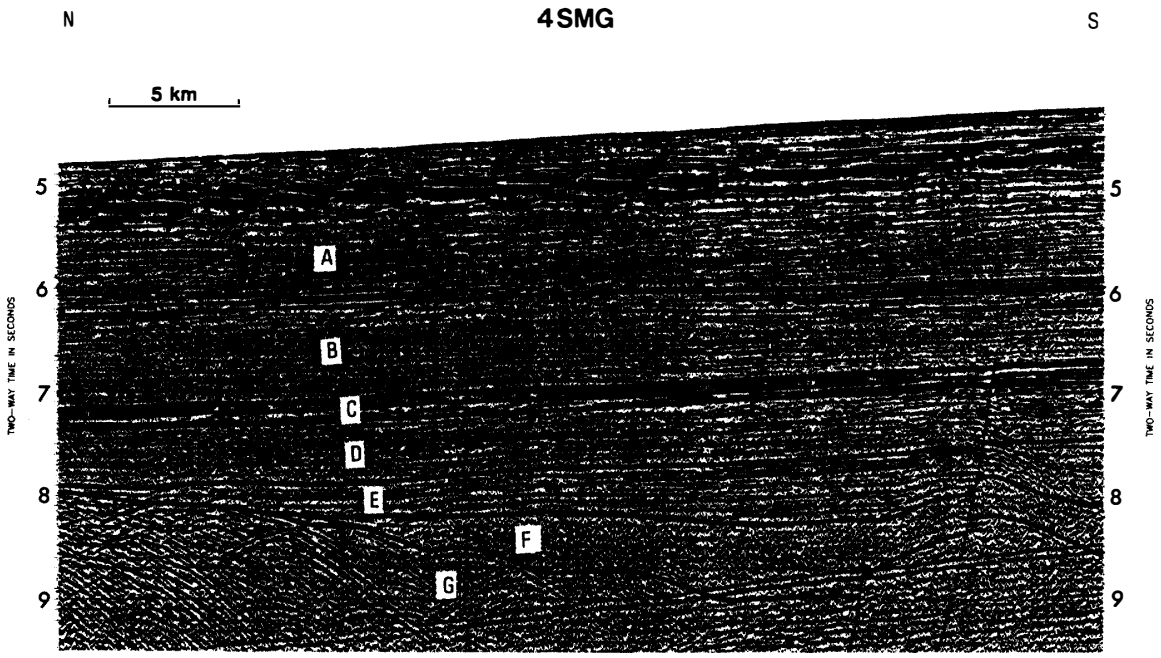

Fig. 8. Seismic profile of the central part of line 4SMG. Wavy reflectors are observed in the upper part of sequence A. Sequence C is characterized by very high amplitude reflectors. Basement G has an oceanic character of strong reflectors with hyperbolic diffraction.

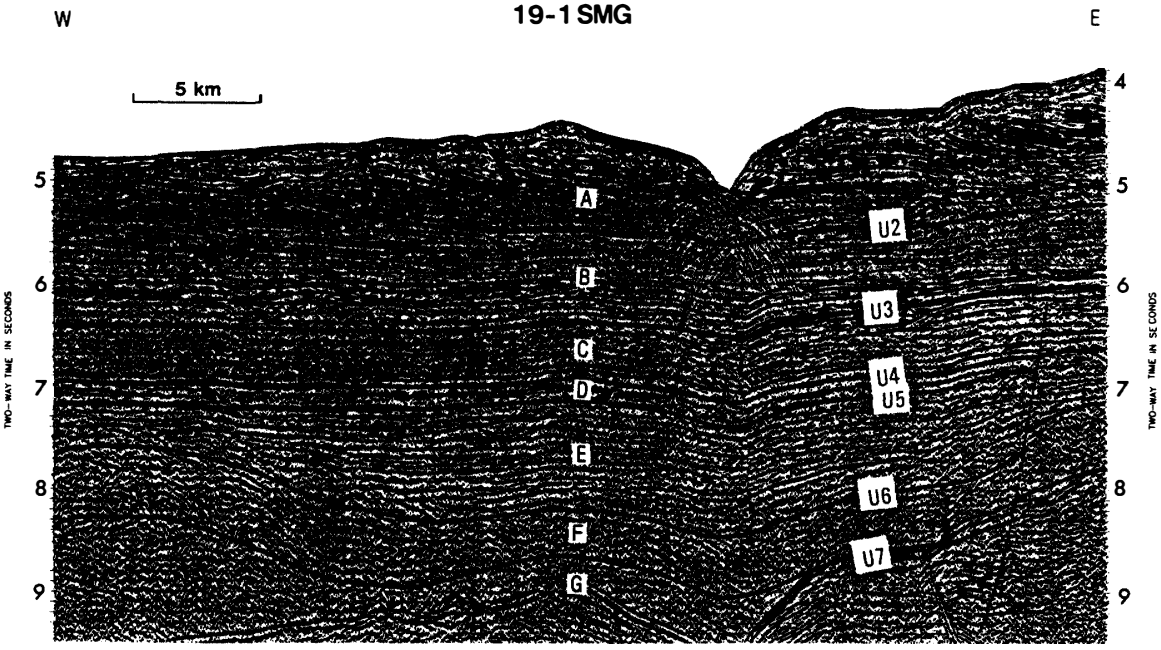

Fig. 9. Seismic profile of the western part of line 19-1SMG. Note erosion in a submarine canyon.

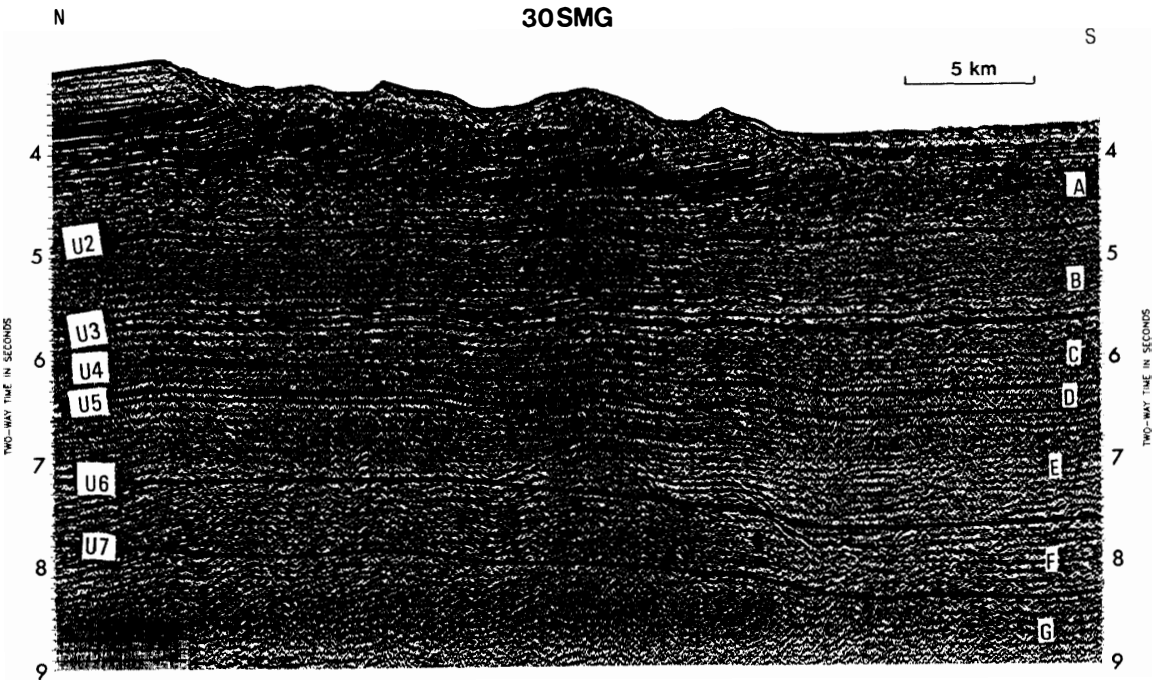

Fig. 10. Seismic profile of the southern part of line 30SMG. Sediments are considered to have been eroded by submarine canyons in the northern and central parts of the profile, while sedimentation by turbidity current possibly occurred in the southern part.

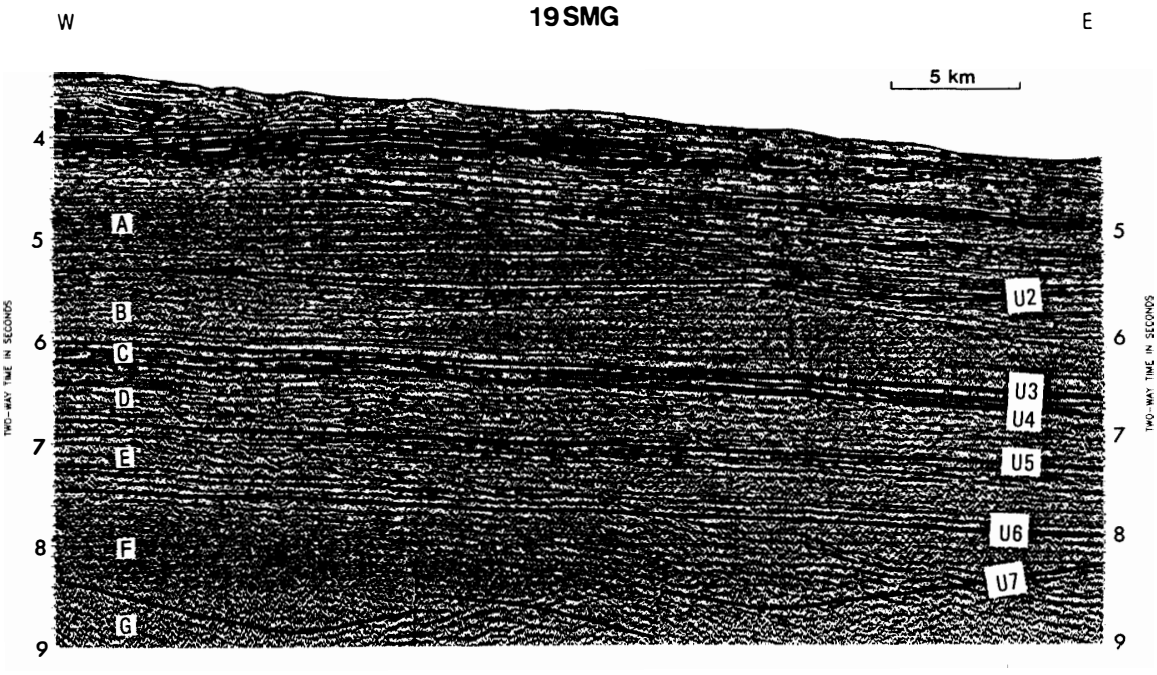

Fig. 11. Seismic profile of the central part of line 19SMG. Note a slumping cutting sequences A and B.

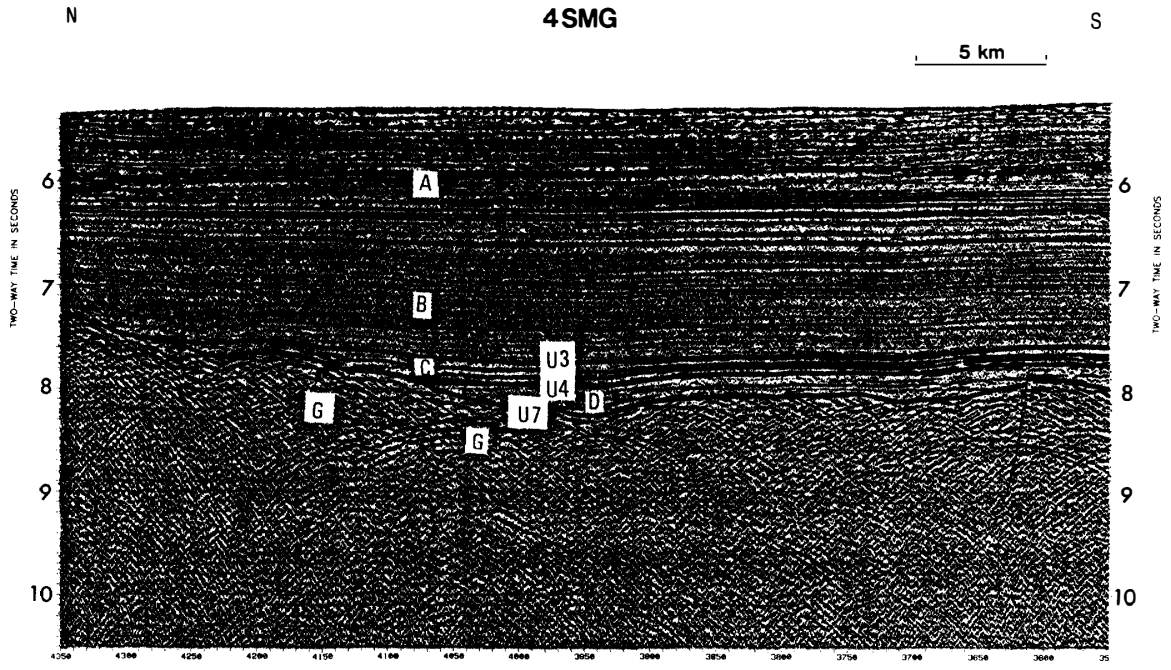

Fig. 12. Seismic profile of the northern end of line 4SMG. Sequences F and E are not observed above the oceanic basement G in this profile, and sequences D and C also diminish in the northern part.

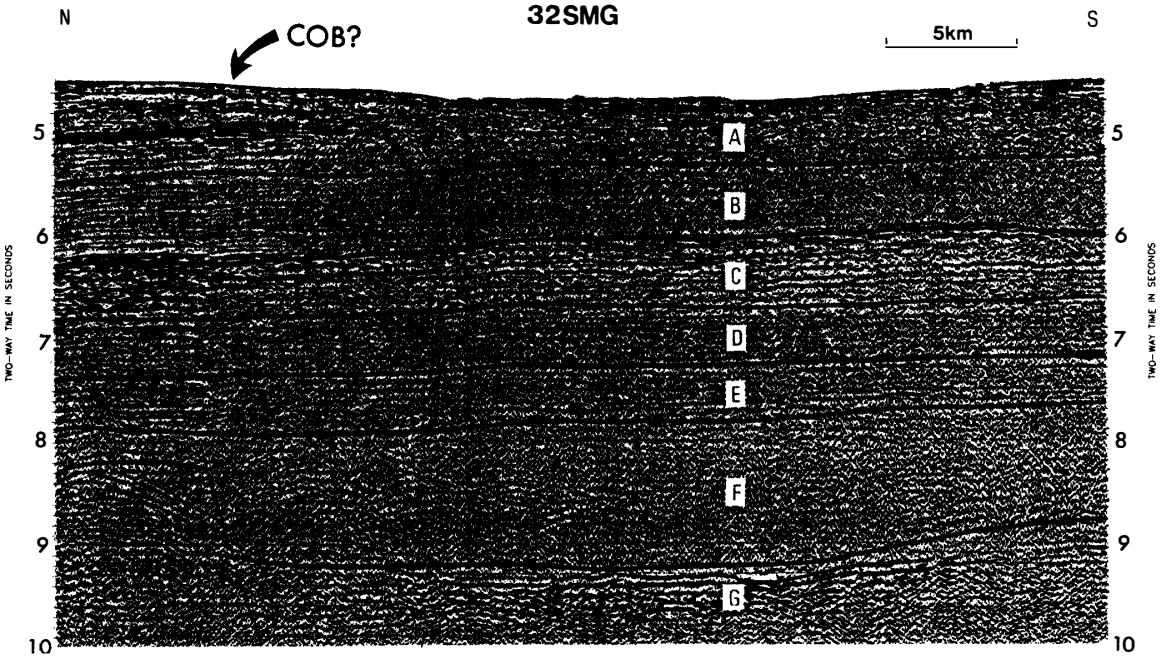

Fig. 13. Seismic profile of the southern part of line 32SMG. The basement G is characterized by low-amplitude reflectors in the southern part of the line, and the fault in the northern part of the profile corresponds to the COB.

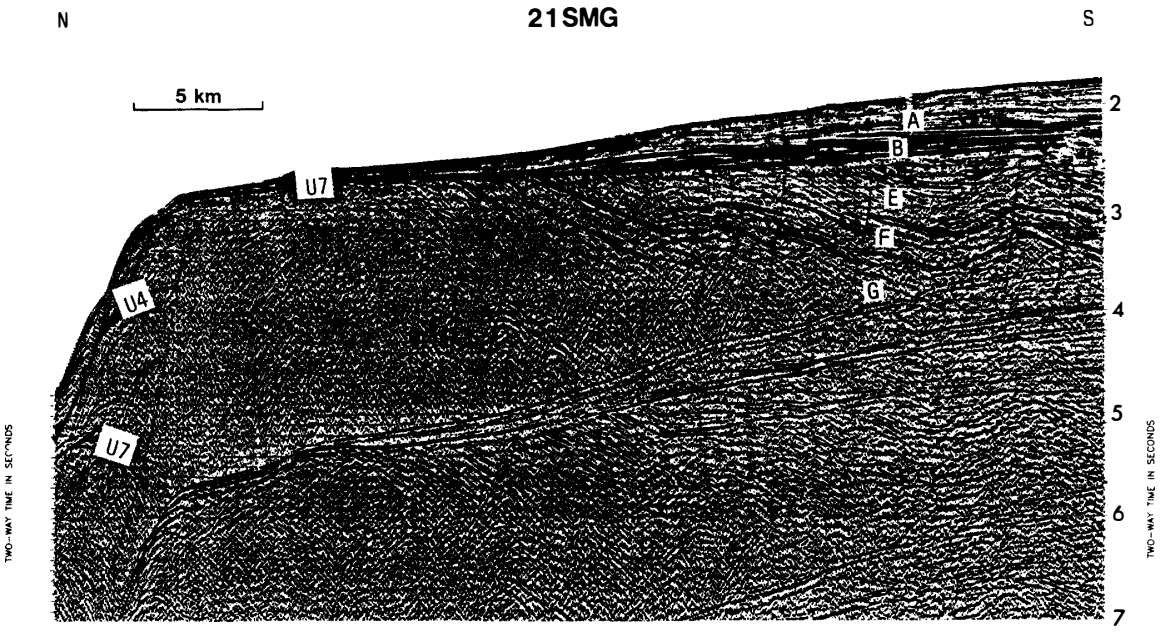

Fig. 14. Seismic profile of the northern part of line 21SMG. Sequences C and D are missing, and the lower sequences E, F and G dip south in this profile.

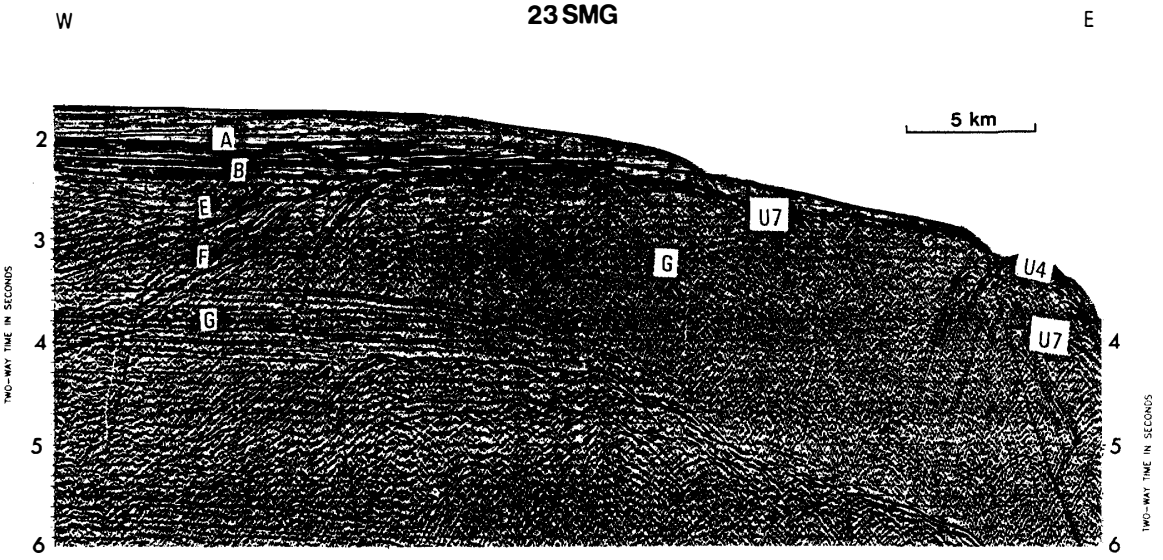

Fig. 15. Seismic profile of the central part of line 23SMG. Sequences C and D are missing, and the lower sequences E, F and G dip west in this profile.

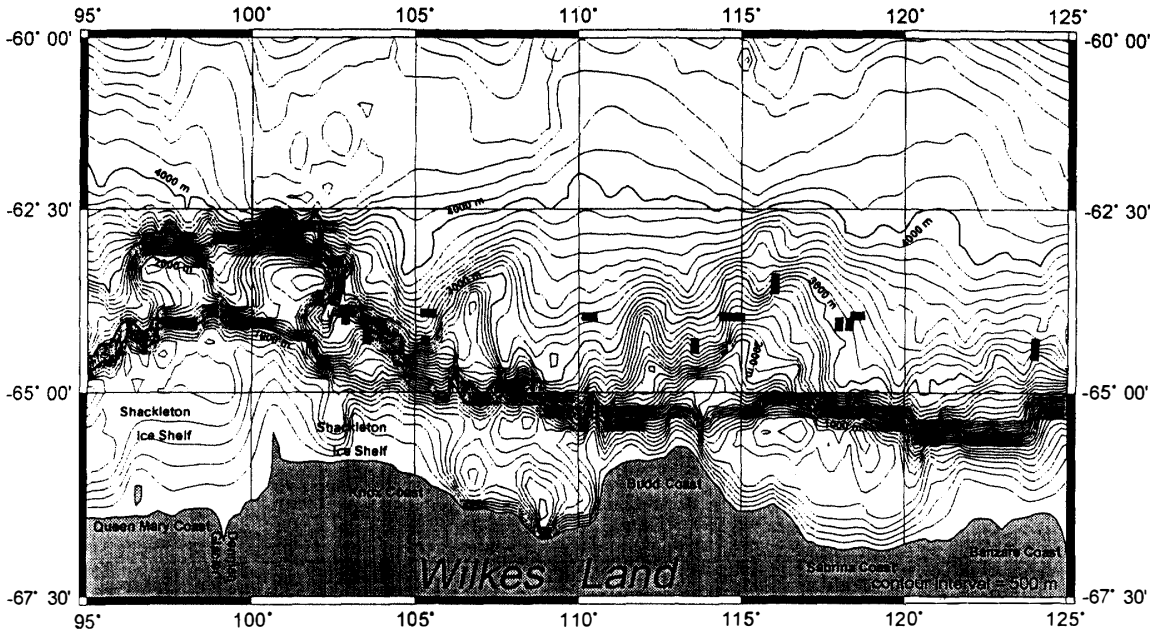

Fig. 16. Distribution of bottom simulating reflectors (BSR) in the survey area based on multichannel and single channel seismic surveys.

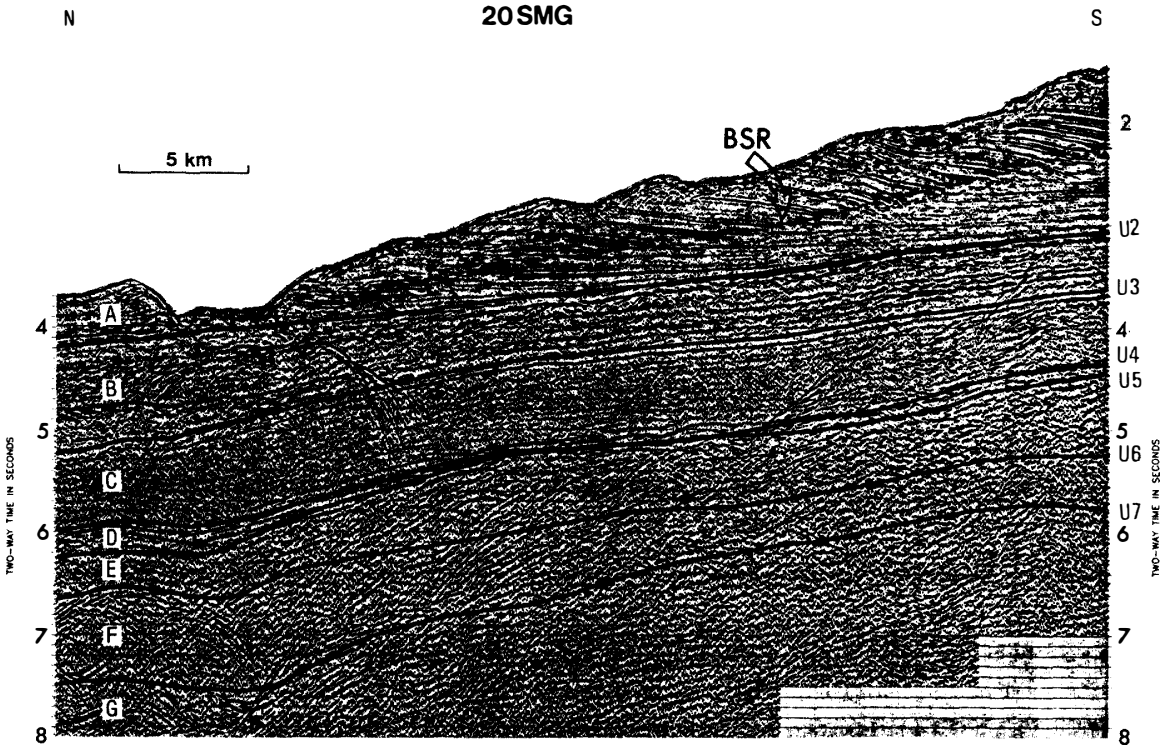

Fig. 17. Seismic profile of the southern end of line 20SMG. A BSR is observed approximately parallel to the sea-bottom and 0.5 to 0.8 s below the bottom in sequence A.

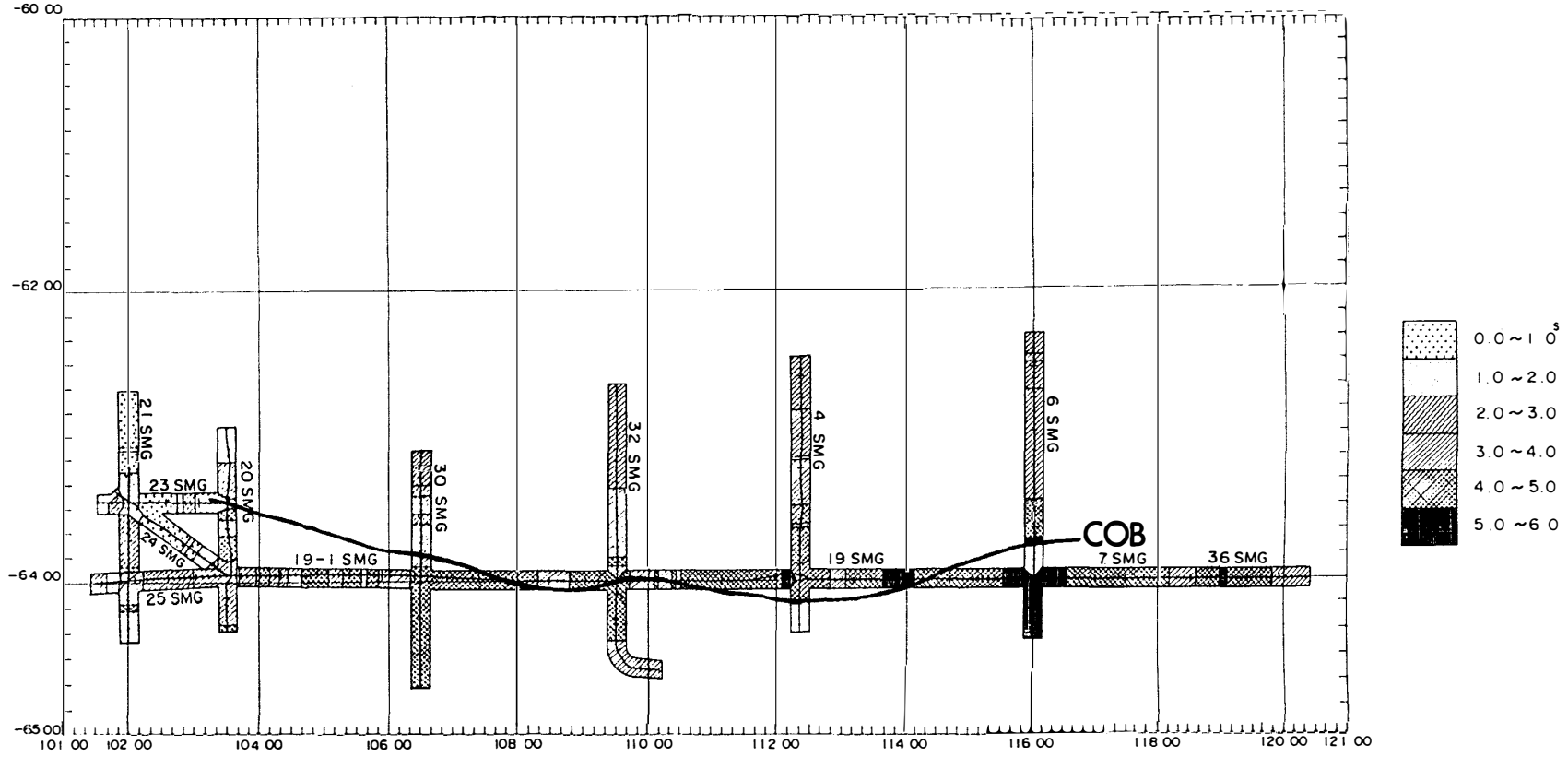

Fig. 18. Total thickness of sediments in s of two-way time based on the multichannel seismic survey. Also shown are the COB inferred from seismic reflection characters of the basement G.

5.2.3. Geological time of the sequences

No well information is available in the survey area other than DSDP site 268, where a 474.5 m-long hole was drilled into sequences A and B (HAYES *et al.*, 1975). Referring to HAMPTON *et al.* (1987) and EITTREIM and SMITH (1987), we tentatively infer the geological time of each sequence as follows (Table 4):

Miocene to Quaternary for sequence A,
Paleocene to Oligocene for sequence B,
Late Cretaceous for sequences C, D and E,
Early Cretaceous for sequence F,
Early Cretaceous and/or older for sequence G landward of COB,
and Cretaceous for sequence G seaward of COB.

5.2.4. Bottom simulating reflectors

Bottom simulating reflectors (BSR) are frequently observed in the continental slope area with depths of 2000 to 3000 m (Fig. 16). They are approximately parallel to the sea bottom, and occur 0.5 to 0.8 s in two-way time below the bottom (Fig. 17). A BSR in this area is not a single continuous reflector but a boundary, where intensities of reflected signals suddenly decrease downward.

6. General Features of Sedimetary Basin

Sediments are thickest around the COB. Total sediment thickness from sequence A to F is greater than 4 s in two-way time in an area extending in the east-west direction along 64°S, and becomes greater than 5 s at about 116°E in the eastern part of the survey area (Fig. 18).

Acknowledgements

The authors are indebted to Capt. T. EBIHARA, officers and crew as well as scientific colleagues of cruise TH-94 for their cooperation and efforts during the preparation and execution of the survey. The authors also thank T. SAKI and an anonymous reviewer for many helpful suggestions for improvement.

References

AKIBA, F. (1982): Late Quaternary diatom biostratigraphy of the Bellingshausen Sea, Antarctic Ocean. Sekiyu Kôdan Sekiyu Kaihatsu Gijutsu Sentâ Kenkyu Hôkoku (Rep. Tech. Res. Cent., J.N.O.C.), **16**, 31–74.

CANDE, S. C. and MUTTER, J. C. (1982): A revised identification of the oldest sea-floor spreading anomalies between Australia and Antarctica. Earth Planet. Sci. Lett., **58**, 151–160.

EITTREIM, S. L. and SMITH, G. L. (1987): Seismic sequences and their distribution on the Wilkes Land margin. The Antarctic Continental Margin: Geology and Geophysics of Offshore Wilkes Land, ed. by S. L. EITTREIM and M. A. HAMPTON. Houston, Circum-Pacific Council for Energy and Mineral Resources, 15–43 (CPCEMR Earth Sci. Ser., 5A).

HAMPTON, M. A., EITTREIM, S. L. and RICHMOND, B. M. (1987): Post-breakup sedimentation on the Wilkes Land margin, Antarctica. The Antarctic Continental Margin: Geology and Geophysics of Offshore Wilkes Land, ed. by S. L. EITTREIM and M. A. HAMPTON. Houston, Circum-Pacific Council for Energy and Mineral Resources, 75–87 (CPCEMR Earth Sci. Ser., 5A).

HAYES, D. E., FRANKES L. A. *et al.* (1975): Site 268. Initial Rep. Deep Sea Drill. Proj., **28**, 153–177.

KIMURA, K. (1982): Geological and geophysical survey in the Bellingshausen Basin, off Antarctica. Nankyoku Shiryô (Antarc. Rec.), **75**, 12–24.

MIZUKOSHI, I., SUNOUCHI, H., SAKI, T., SATO, S. and TANAHASHI, M. (1986): Preliminary report of geological and geophysical surveys off Amery Ice Shelf, East Antarctica. Mem. Natl Inst. Polar Res., Spec. Issue, **43**, 48–61.

OKUDA, Y., YAMAZAKI, T., SATO, S., SAKI, T. and OIKAWA, N. (1983): Framework of the Weddell Basin inferred from the new geophysical and geological data. Mem. Natl Inst. Polar Res., Spec. Issue, **28**, 93–114.

SAKI, T., TAMURA, Y., TOKUHASHI, S., KODATO, T., MIZUKOSHI, I. and AMANO, H. (1987): Preliminary report of geological and geophysical surveys off Queen Maud Land, East Antarctica. Proc. NIPR Symp. Antarct. Geosci., **1**, 23–40.

SANDWELL, D. T. and SMITH, W. F. (1992): Global marine gravity from ERS-1, Geosat, and Seasat reveals new tectonic fabric. EOS; Trans., **73**, 133.

SATO, S., ASAKURA, N., SAKI, T., OIKAWA, N. and KANEDA, Y. (1984): Preliminary results of geological and geophysical surveys in the Ross Sea and in the Dumont D'urville Sea, off Antarctica. Mem. Natl Inst. Polar Res., Spec. Issue, **33**, 66–92.

SHIMIZU, S., MORISHIMA, H. and TAMURA, Y. (1989): Preliminary report of geophysical and geological surveys off the South Orkney Islands, Scotia Arc region. Proc. NIPR Symp. Antarct. Geosci., **3**, 52–64.

TSUMURAYA, Y., TANAHASHI, M., SAKI, T., MACHIHARA, T. and ASAKURA, N. (1985): Preliminary report of the marine geophysical and geological surveys off Wilkes Land, Antarctica in 1983–1984. Mem. Natl Inst. Polar Res., Spec. Issue, **37**, 48–62.

VEEVERS, J. J. (1987): The conjugate continental margins of Antarctica and Australia. The Antarctic Continental Margin: Geology and Geophysics of Offshore Wilkes Land, ed. by S. L. EITTREIM and M. A. HAMPTON. Houston, Circum-Pacific Council for Energy and Mineral Resources, 45–73 (CPCEMR Earth Sci. Ser., 5A).

WESSEL, P. and SMITH, W. H. F. (1991): Free software helps map and dispaly data. EOS; Trans., **72**, 441 & 445–446.

YAMAGUCHI, K., TAMURA, Y., MIZUKOSHI, I. and TSURU, T. (1988): Preliminary report of geophysical and geological surveys in the Amundsen Sea, West Antarctica. Proc. NIPR Symp. Antarct. Geosci., **2**, 55–67.

(Received March 25, 1996; Revised manuscript accepted July 11, 1996)